Egyptian Geophysical Society
EGS Journal, Vol. 10, No. 1, 65-72 (2012)

VELOCITY IMAGING OF THE NEAR-SURFACE STRUCTURES BY DIVING-WAVE TOMOGRAPHY, DIVING-WAVE PENETRATION CORRECTION AND CONVENTIONAL REFRACTION ANALYSES

A. El-Werr[(1)] and H. Almalki[(2)]

(1) Geophysics Department, Faculty of Science, Ain Shams University, Abbasia, Cairo, Egypt.
(2) King Abdulaziz City for Science and Technology, Riyadh, KSA.

تصوير السرعة فى التراكيب الضحلة بواسطة تحاليل تصوير الموجة الغاطسة،

وتصحيح اختراق الموجة الغاطسة والانكسار التقليدى

الخلاصة: يتناول هذا البحث استخدام البيانات السيزمية عبر أحد القطاعات لانشاء صورة السرعة وبناء نموذج السرعة تحت هذا القطاع بتطبيق نظريات مختلفة. وأبسط هذه النظريات هو التحليل الانكسارى التقليدى الذى يفترض قيمة ثابتة لمتوسط السرعة فى كل طبقة. أما المفهوم الثانى فهوتصوير الموجة الغاطسة أو التصوير الانكسارى الذى طبق لتصوير السرعة عبر نفس القطاع السابق ذكره مفترضا زيادة خطية للسرعة مع العمق. والمفهوم الثالث هو تطبيق تصحيح اختراق الموجة الغاطسة وإنشاء صورة السرعة لطبقة التربة ثابتة السرعة ولصخر الأساس المتدرج رأسيا فى السرعة. وتم انجاز مقارنة بين هذه المفاهيم الثلاثة لتبين مدى توافق صور السرعة بينهم.

وتم أيضا انشاء منحنيات السرعة مع العمق لتعكس الزيادة الخطية فى السرعة مع العمق. ولوحظ وجود زيادة سريعة للسرعة مع العمق فى الجزء الضحل من صخر الحجر الجيرى المتدرج السرعة رأسيا يتبعه تدرج صغير فى السرعة فى الأعماق الكبيرة. وأخيرا تم حساب المدلولات السيزمية لتعيين جودة المادة لصخر الأساس المتدرج السرعة رأسيا. واستنتج أيضا وجود جزء ضحل متأثر بشدة بعوامل التجوية من صخر الحجر الجيرى وهذا ما تم تأكيده من نتائج الحفر بالمنطقة.

ABSTRACT: *In this paper, seismic refraction data obtained along a single profile was used to construct a velocity image and to build up a velocity model beneath it by applying different approaches. The simplest one is the conventional refraction analysis or layer refraction which assumes an average constant velocity value for each layer. The second approach is the diving-wave tomography or refraction tomography that has been applied for velocity imaging along the same profile assuming a linear continuous increase of velocity with depth. The third algorithm is the application of the diving-wave penetration correction and construction of a velocity image for the constant velocity soil layer and the vertical velocity gradient bedrock. A comparison between the results of these three approaches has been carried out to show the velocity concurrence of their images.*

Velocity-depth model curves have also been established to reflect the linear increase of the velocity with depth. A rapid velocity increase with depth within the shallower part of the vertical velocity gradient limestone bedrock followed by a smaller velocity gradient at greater depths can be noticed. Finally, seismic parameters have been calculated for estimation of the rock material quality of the vertical velocity gradient bedrock. It is concluded that an intensively or completely weathered shallower part of the limestone bedrock exists which is confirmed by the drilling results.

INTRODUCTION

Three different techniques have been applied to construct a seismic velocity image along a single profile at King Abdulaziz City for Science and Technology (KACST), Riyadh, KSA. Conventional refraction analysis or layer refraction, diving-wave tomography, also known as refraction tomography or turning-ray tomography and diving-wave penetration correction approaches have been applied for velocity imaging. This study aims at the estimation of the near-surface geology for civil engineering purposes. A comparison between the velocity imaging constructed from these three techniques was also done to find out the degree of matching between them. Exploratory borings for determination of the soil profile layer thicknesses and lithological description were used supporting the seismic data analysis.

EXPLORATORY BORINGS

The results of the exploratory borings (Soil & Foundation Co. Ltd., 2007) along the interpreted profile were used to support the seismic data analysis. The estimated layer thicknesses and lithological description in the study area are the following: (1) a first layer composed of brown, dense, dry silty sand with gravel with a thickness range of 1.5-4.8 m, (2) a second layer composed mainly of completely weathered limestone with an average thickness of 6.5 m, and (3) the third layer is formed of moderately weathered limestone.

SEISMIC DATA ANALYSIS

There are three different approaches used in this work aiming at a construction of a seismic velocity image from each approach and finally making a

comparison between them to indicate the velocity concurrence between them.

(1) Conventional Refraction Analysis:

In the conventional refraction analysis the shallower part of the geological section is described as layers wherein velocities change very smoothly but very sharply at the boundaries between the layers. In-line spread layout was conducted along the interpreted profile for generation of compressional seismic waves. The total interpreted seismic profile length is 132 m with 2 m geophone interval. Seven shot points were located at the following distances: -9, 0, 32, 64, 100, 132 and 141 m constituting two end-on shots (0 and 132 m), two offset shots (-9 and 141 m) and three split-spread shots (32, 64 and 100 m). A hydraulic weight drop was used as a source of seismic energy vertically hitting a steel striker plate. The generated seismic energy was measured by a 14 Hz vertical geophone and recorded by a multi-channel signal enhancement Seismograph of Geometrics Inc. (Geode and Strata Visor NZ Model). Some selected shot records (seismograms) are shown in Fig. 1.

An advanced SeisImager Software Package (Geometrics Inc., 2005) has been used for seismic data processing sequence. Traveltime-distance curves are established along the acquired profile (Fig. 2). First-break picking and layer assignment were done for each segment on the traveltime-distance curves, and finally, the velocity-depth image along this profile has been constructed showing average velocity values 687, 1383 and 4428 m/s for the first, second and third layers, respectively as shown in Fig. 3 with average thicknesses 2.5 and 7.5 m for both of the first and second layers, respectively.

(2) Diving-Wave Tomography:

Several literature explained diving-wave tomography, also known as refraction traveltime tomography or turning-ray tomography which uses first-arrival traveltime as input data (e.g. Zhu and McMechan, 1989; Zhu, et al. 1992; Stefani, 1995; Zhu, et al. 1998; Osypov, 1999; Osypov, 2000; Osypov, 2001; Zhu, et al. 2001; Zhu, 2002; Speece, et al. 2003; Kanli, 2008 & 2009; Kanli, et al 2008; Teimoornegad and Poroohan, 2007 & 2008; Miller, et al. 2005).

Seismic tomography is usually formulated as an inverse problem. It is a seismic imaging technique for estimating the compressional wave velocity. Several methods have been developed for this purpose, e.g. refraction traveltime tomography, finite-frequency traveltime tomography, reflection traveltime tomography and waveform tomography. In refraction traveltime tomography, the observed data are the first-arrival traveltimes t and model parameters are the slowness S. The forward problem can be formulated as $t = LS$, where L is the forward operator which, in this case, is the raypath matrix. The solution involves minimization of the difference between the observed traveltimes and those predicted (calculated) by ray tracing through an initial model. Zhu (2002) explained five steps for that iterative solution: (1) picking of first-arrivals, (2) ray tracing through an initial estimate of the velocity model, (3) segmenting raypaths into the portion contained in each cell of the velocity model, (4) computing the differences between the observed and predicted traveltimes for each ray, and (5) iteratively back projecting the time differences to produce velocity-model updates. Velocity updates are performed by a simultaneous iterative reconstruction technique (SIRT).

In the present study, seismic tomography profile was conducted along the same location of the conventional profile. Geophone interval was also 2 m and the shot points were moved along the profile and shot at each geophone location, i.e. shot interval = geophone interval = 2 m. The total number of shots was 77 shots, the total number of geophones was 75 and the number of stacks was 3 for each shot. The traveltime-distance curves along the interpreted profile produced from each shot are shown in Fig. 4.

SeisImager Software Package was also used for processing steps of the seismic tomography traveltime-distance curves. The final result is a velocity image along the interpreted profile (Fig. 5). The velocity image shows the following features: deeper depth values till 40 m, color scale of the velocity image range from 380 m/s to 5000 m/s, and a better image enhancement than conventional refraction analysis. This tomography velocity image or tomogram is very useful during the construction of the high-rise or tall-buildings and establishment of the modern seismic design building codes.

(3) Diving-Wave Penetration Correction Algorithm:

In this paper, we have an ideal case study of constant soil layer velocity of the first layer (about 600 m/s) overlying bedrock with a continuous velocity increase with depth. Small velocity values around 1000 m/s are found at the top surface of this limestone bedrock due to the effect of strong weathering processes which decrease with depth. As the weathering and fracturing processes gradually decrease with depth, the seismic velocity increases gradually and continuously as well. This medium can be considered as a vertical velocity gradient medium and the velocity-depth distribution V=V(z) can be expressed by linear, parabolic, exponential or any other velocity function. Seismic waves propagate in this medium according to Snell's law along curved trajectories, returning back to the ground surface. This kind of waves are called diving waves and they can be demonstrated by the convergence of their overtaking traveltime-distance curves. The depth within this medium can be determined according to Wiechert-Herglotz-Bateman equation (Slichter, 1932) by using only single traveltime-distance curve. However, in our study we used each pair of reversed traveltime-distance curves for depth determination by an equation modified for linear velocity function.

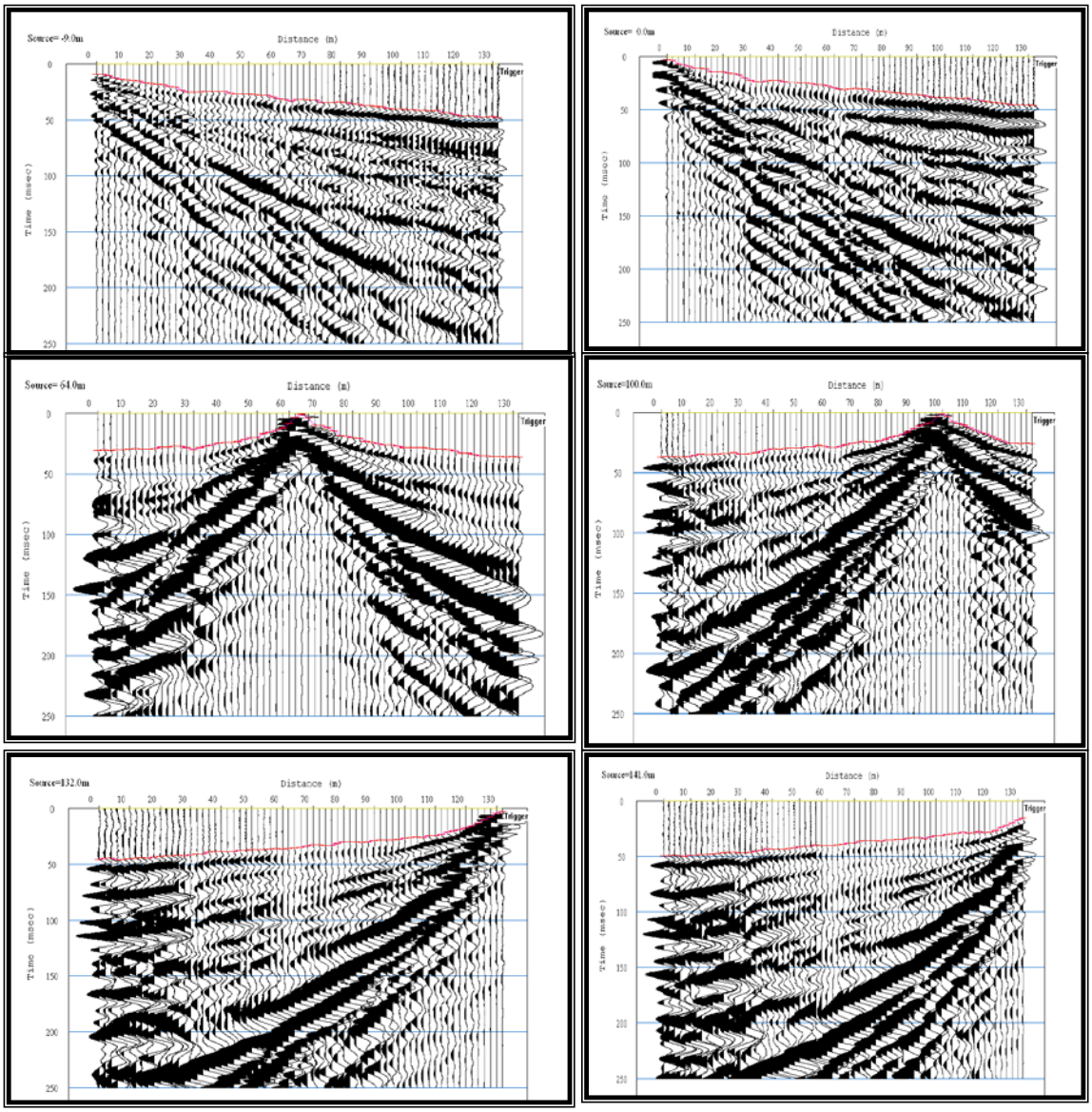

Fig. (1): Examples of shot records for conventional refraction analysis.

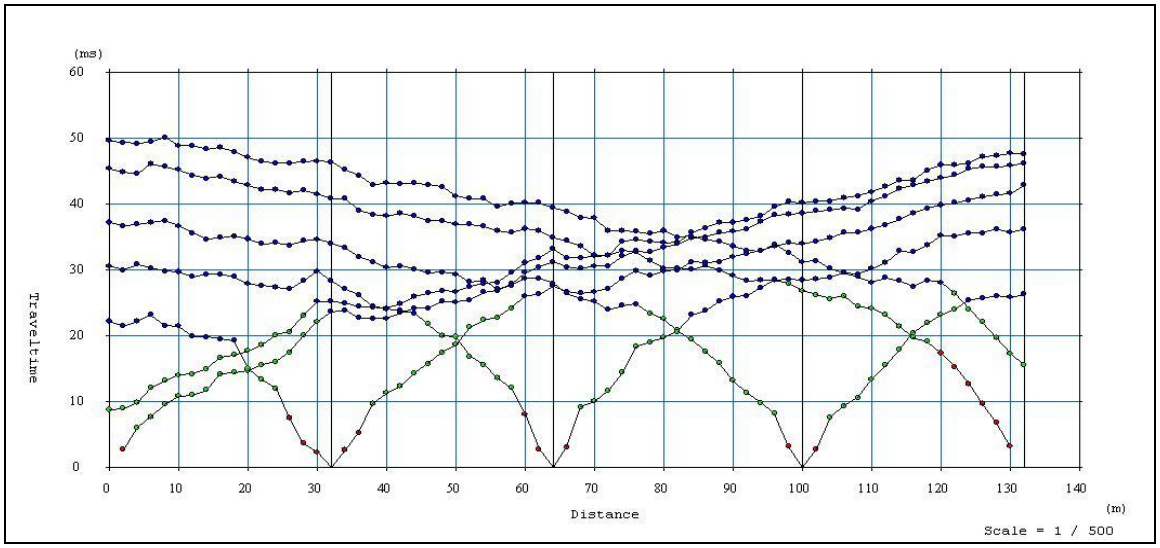

Fig. (2): Traveltime-distance curves along the studied profile.

There have been many theoretical studies disclosed that seismic wave velocities within layers are not constant (see, Rubey, 1927; Terzaghi, 1940; Faust 1953; Gassman, 1951; Jankowsky, 1970, Gurvich, 1972; Greenhalgh, 1976; Greenhalgh et al., 1980; Greenhalgh and King, 1981; Skopec, 1981 & 1989; Skopec and El-Werr, 1996; El-Werr and Skopec, 1996; and El-Werr, 1999a & 1999b).

All interpretational methods are designed only for using head waves. However, in our case, the existence of diving-wave is very remarkable from the convergence of their overtaking traveltime-distance curves (Fig. 6). For this reason, diving-wave traveltimes should be transformed into traveltimes of head waves by introducing a diving-wave penetration correction. If we do not introduce this correction, the results will bear errors in depth and velocity determinations at the surface of the bedrock.

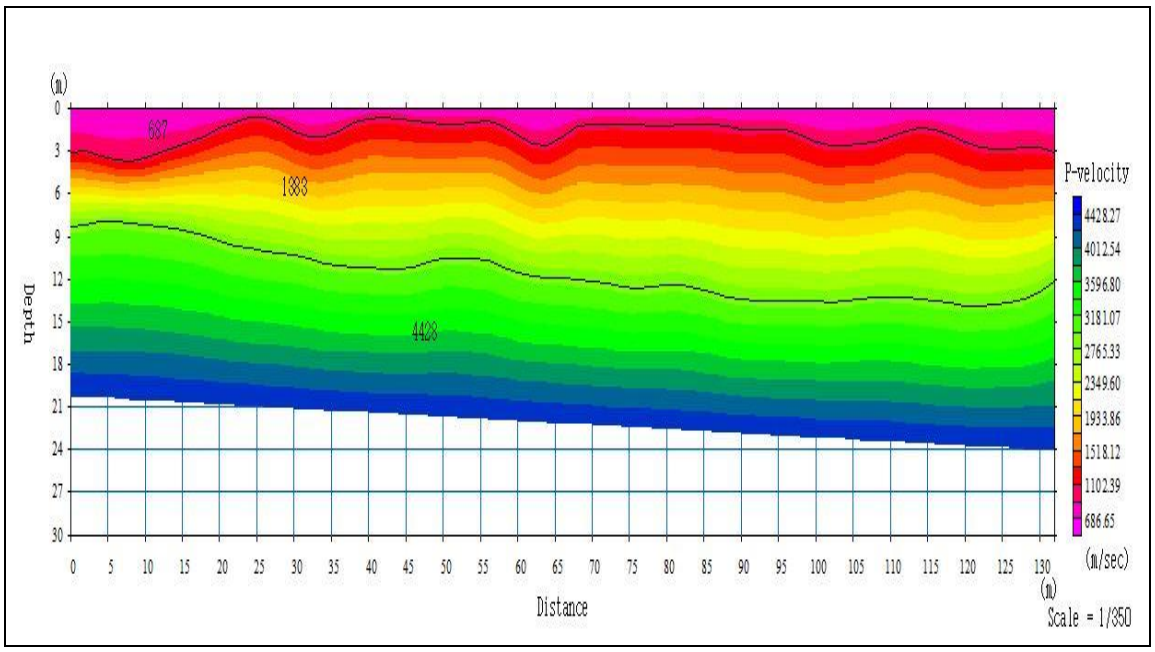

Fig. (3): Velocity image constructed from conventional refraction analysis.

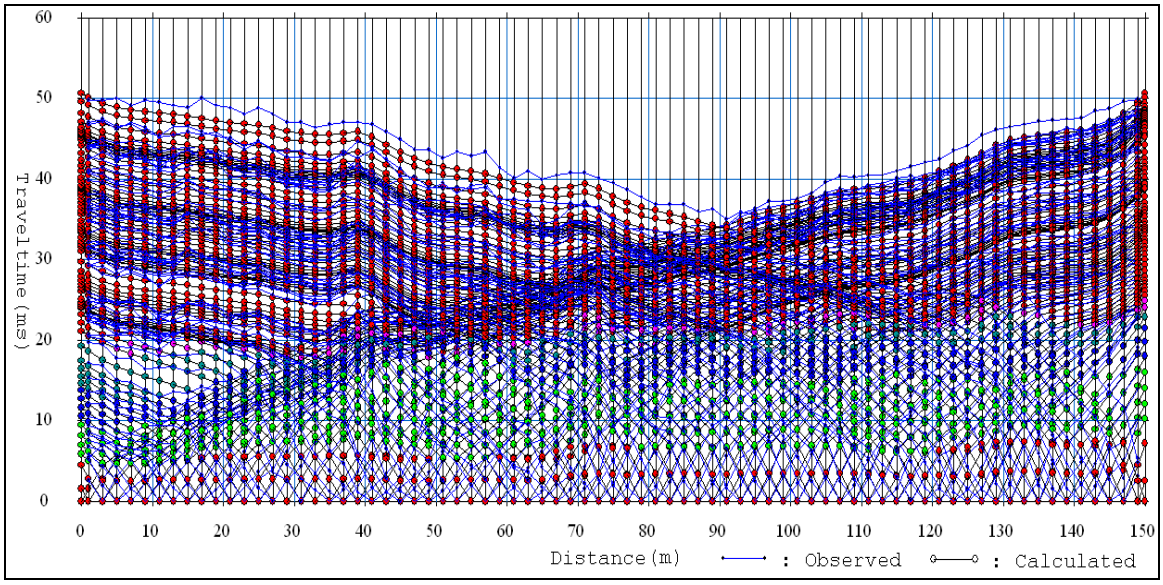

Fig. (4): Traveltime-distance curves for diving-wave tomography.

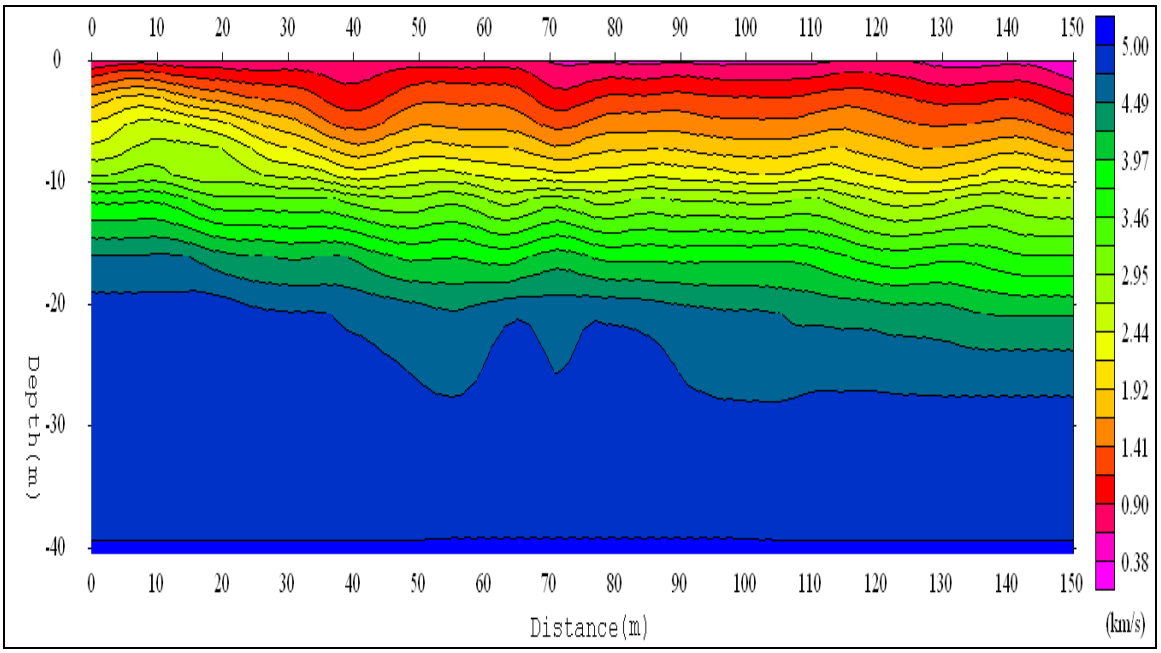

Fig. (5): Velocity image constructed from diving-wave tomography analysis.

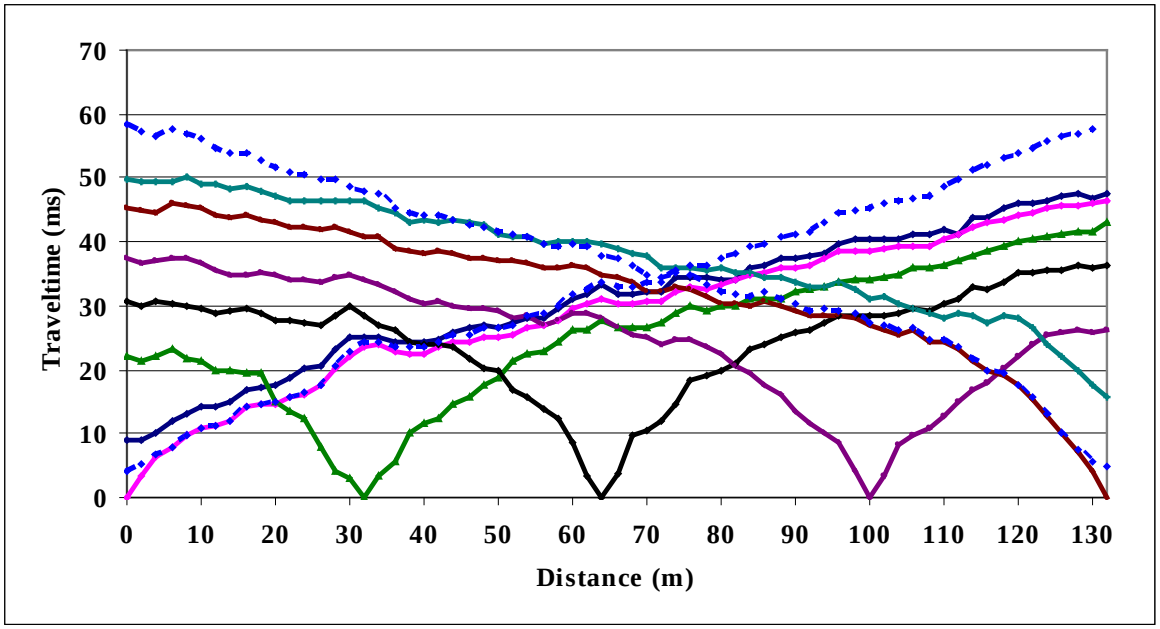

Fig. (6): Traveltime curves of diving-waves (solid lines), corrected times of head waves (dashed lines).

The velocity image constructed from this approach (Fig. 7) shows a constant soil layer velocity (600 m/s) of silty sand with a thickness range of 1.6-4.5 m overlying a completely weathered limestone with a gradual increase of velocity with depth.

The velocity at the top surface of the bedrock is about 1000 m/s for the completely weathered limestone while it attains more than 5000 m/s for intact massive limestone at depth of 25 m.

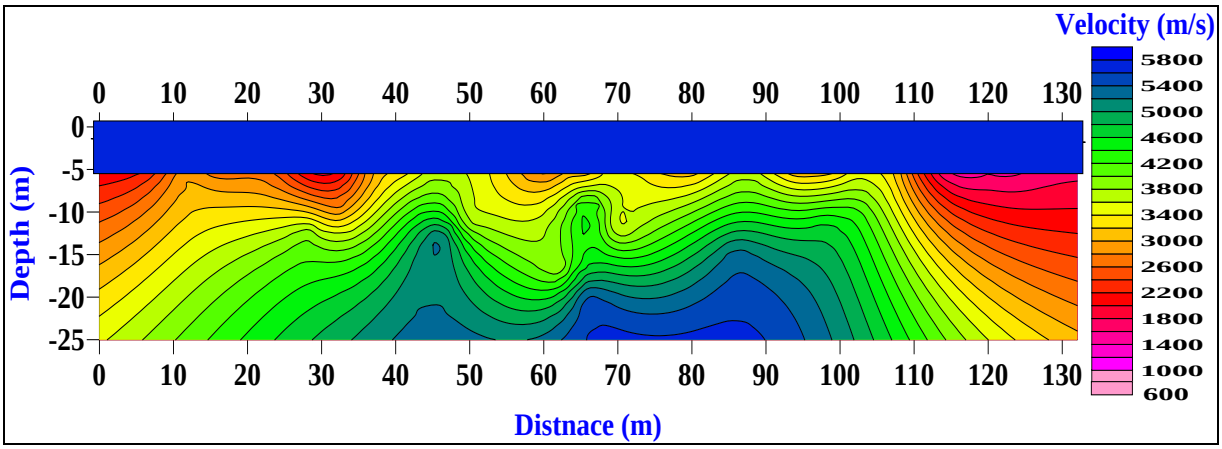

Fig. (7): Velocity image constructed from diving-wave penetration correction approach.

(4) Velocity Models Construction:

New buildings are planned to be constructed in the near-future of the study area. In addition to the aforementioned velocity imaging, velocity models represented by velocity at each depth will help to a great extent during construction of these buildings. Three velocity models are established along the studied profile. The first velocity model (Fig. 8) is established from the results of the conventional refraction analysis which assumes almost constant average velocity values 687, 1383 and 4428 m/s for the first, second and third layers, respectively, with thicknesses about 2.5 and 10 m for the first and second layers, respectively. The second velocity model is established from the diving-wave tomography (Fig. 8). The velocity model of the diving-wave tomography shows small velocity value (380 m/s) for the first silty sand layer, then an intensive weathered limestone bedrock with a velocity at its surface around 1000 m/s which increases rapidly with a large vertical velocity gradient till it reaches 4250 m/s at depth of about 17.5 m, and finally the velocity increases slightly to 5000 m/s at depth about 40 m. The third model is constructed from the data analysis of the diving-wave penetration correction approach (Fig. 8). It shows constant first layer velocity (600 m/s) overlying completely weathered bedrock with lower velocity (about 1000 m/s) at its top surface with rapid velocity increase with depth of large gradient till it reaches about 4500 m/s at depth 17 m, followed by slight velocity gradient within the intact massive limestone where the velocity attains more than 5000 m/s at depth 25 m.

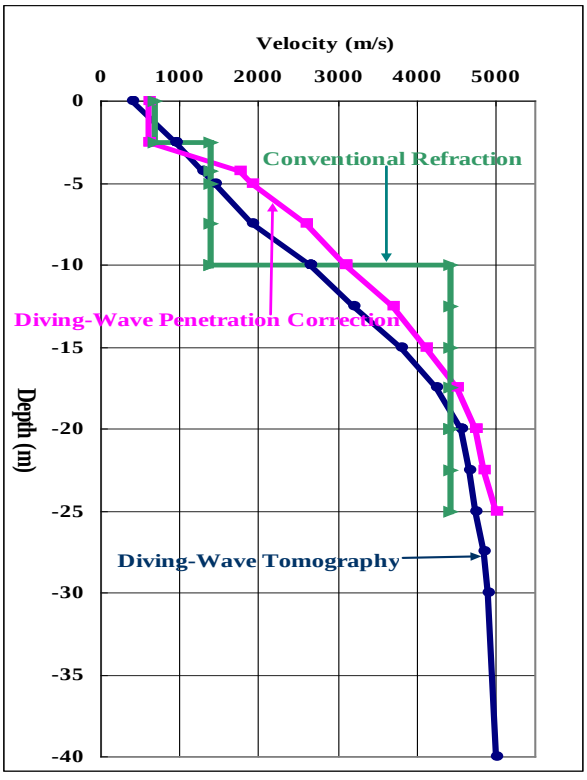

Fig. (8): Velocity models constructed from the three different approaches

(5) Rock Quality Estimation from Seismic Parameters

Seismic parameters in the form of velocity increment ($\Delta V / \Delta Z$), weighted velocity gradient ($V_G = V^{-}.\Delta V / \Delta Z$) and velocity gradient $K = (V(Z) - Vo)) / Vo.Z$ have been calculated at x-co-ordinate 30 m for the second and third approaches, where V^{-} is the mean velocity of two *V(Z)* values with difference ΔV at two successive depths within a depth interval ΔZ, *Vo* is the velocity at the top surface of the bedrock. These parameters are found to be more close to each other from these two approaches and they are equal to 236 S^{-1}, 573 $x10^{\wedge 3}$ mS^{-2} and 0.077 m^{-1} for the velocity increment, weighted velocity gradient and velocity gradient, respectively. These seismic parameter values are large enough to document limestone bedrock with good material quality which is suitable for building as a foundation layer.

CONCLUSIONS

Conventional refraction analysis, diving-wave tomography and diving-wave penetration correction have been carried out along a single profile to construct a velocity image of the constant soil layer velocity and the vertical velocity gradient bedrock. A comparison between the results of these three approaches has been done to test them together with each other and to indicate their reliability that was confirmed by exploratory boreholes. A velocity concurrence between the three obtained images has been noticed.

Also, velocity model curves have been established to reflect the amount of the linear increase of the velocity with depth. A rapid velocity increase with depth within the shallower part of the vertical velocity gradient limestone bedrock followed by a slight velocity gradient at greater depths has also been observed. For estimation of the rock material quality, seismic parameters have been calculated for the vertical velocity gradient bedrock. It was found out that seismic parameters are large enough to document a bedrock with good material quality in spite of its highly degree of weathering.

It can be concluded that a good matching is found between the results of the applied three approaches particularly the second and third ones, which we consider much better than the first approach. This kind of diving-wave analysis for velocity imaging is very useful and it is recommended for tall-buildings construction and establishment of the modern seismic design building codes.

REFERENCES

El-Werr, A. and Skopec, J., 1996, Convergency of time-distance curves in seismic refraction and its interpretation in gradient medium: 56 Jahrestagung der Deutschen Geophysikalischen Gesellschaft (DGG), Freiberg, Germany.

El-Werr, A., 1999a, Shallow seismic investigations of inhomogeneous media: 17th Ann. Mtg. of the Egyptian Geophysical Society, p. 203-232.

El-Werr, A., 1999b, Determination of vertical velocity gradient from seismic refraction data using master curves matching method: The 1st Internat. Conference on the Geology of Africa, Assiut, Egypt, v. 1, p. 525-536.

Faust, L. Y., 1953, A velocity function including lithologic variation: Geophysics, v. 18, p. 271-288.

Geometrics Inc., 2005, SeisImager software package.

Gassman, F., 1951, Elastic waves through a packing of spheres: Geophysics,v. 16, p. 673-685.

Greenhalgh, S. A., 1976, Seismic refraction studies in variable velocity media: M. Sc. Thesis, University of Sydney, 258 p.

Greenhalgh, S. A., King, D. W., and Emerson, D. W., 1980, On the fitting of velocity functions to seismic refraction data: Bull. Australian Soc. of Explor. Geophysics (in press).

Greenhalgh, S. A., and King, D. W., 1981, Curved raypath interpretation of seismic refraction data: Geophysical Prospecting., v. 29, p. 853-882.

Gurvich, I. I., 1972, Seismic prospecting: Mir Publications, Moscow, 462 p.

Jankowsky, W., 1970, Empirical investigation of some factors affecting elastic wave velocities in carbonate rocks: Geophysical Prospecting, v. 18, p. 103-118.

Kanli, A. I. 2008, Image reconstruction in seismic and medical tomography: Journal of Environmental & Engineering Geophysics, v. 13, n. 2, p. 85-97.

Kanli, A. I. 2009, Initial velocity model construction of seismic tomography in near-surface applications: Journal of Applied Geophysics, v. 67, p.52-62.

Kanli, A. I., Pronay, Z., Miskokzi, R., 2008: The importance of the special system geometry on the image reconstruction of seismic tomography: Journal of Geophysics and Engineering, v. 5, p. 77-85.

Miller, C. R., Allen, A. L., Speece, M., El-Werr, A., and Link, C. A., 2005: Land streamer aided, geophysical studies at Saqqara, Egypt, Journal of Environmental and Engineering Geophysics (JEEG), Environmental & Engineering Geophysical Society, Denver, USA, V.10, No. 4, P. 371-380.

Osypov, K., 1999, Refraction Tomography without ray tracing: 69th Ann. Internat. Mtg., Soc. Explor. Geophys., p. 1283-1286.

Osypov, K., 2000, Robust refraction tomography: 70th Ann. Internat. Mtg., Soc. Explor. Geophys., p. 2032-2035.

Osypov, K., 2001, Refraction Tomography: A practical overview of emerging technologies: February Technical Luncheon, CSEG Recorder, p. 5-8.

Rubey, W.W., 1927 The effect of gravitational compaction on the structure of sedimentary rocks: Bull. AAPG., v. 11, p. 621.

Skopec, J, 1981, Introduction of correction for the penetration of rays in shallow seismic prospecting: Acta Univ. Carol. Geol., Prague, n. 1, p. 53-69.

Skopec, J., 1989, Shallow seismic investigations of the vertical velocity gradient media: Acta Univ. Carol. Geol., Prague, n. 3, p. 393-408.

Skopec, J. and El-Werr, A., 1996: The use of convergency for estimating the correction of penetrating seismic waves: Acta Univ. Carol. Geol., Prague, n. 40, p. 13-20.

Slichter, L. B., 1932, Interpretation of seismic travel-time curves in horizontal structures: Physics, v. 3, p. 273-295.

Soil and Foundation Co. Ltd, 2007. Geotechnical investigation report for the proposed KACST project.

Speece, M.A., Miller, C.R., El-Werr, A.K., and Link, C.A., 2003, Land streamer aided, seismic diving-wave tomography at an archaeological site, Saqqara, Egypt: 73rd Ann. Internat.Mtg., Soc. Expl. Geophys., Expanded Abstracts, 1255–1258.

Stefani, J. P., 1995, Turning-ray tomography: Geophysics, v. 60, p. 1917-1929.

Teimoornegad, K. and Poroohan, N., 2007, Application of seismic tomography techniques in dam site: International Journal of Geology, Issue 3, v. 1, p. 61-69.

Teimoornegad, K. and Poroohan, N., 2008, Hidden fault location in Nimroud dam site using seismic tomography: Proc. Of the WSEAS International Conf. New Aspects of Engineering Mechanics, Structure, Engineering Geology, Heraklion, Crete Island, p. 246-251.

Terzaghi, K., 1940, Compaction of lime mud as a cause of secondary structure: Journal of Sedimentary Petrology, v. 10, p. 78-90.

Zhu, X., and McMechan, G. A., 1989, Estimation of two-dimentional seismic compressional-wave velocity distribution by iterative tomography imaging: Internat. J. Imag. Sys. Tech., v. 1, p. 13-17.

Zhu, X., Sixta, D. P., and Angstman, B. G., 1992, Tomostatics: Turning-ray tomography + statics corrections: The Leading Edge, v. 11, n. 12, p. 15-23.

Zhu, X., 2002, Velocity imaging through complex near-surface structures by tomography: EAGE 64th Conference & Exhibition- Florence, Italy.

Zhu, X., Angstman, B. G., and Sixta, D. P., 1998, Overthrust imaging with tomo-datuming: Geophysics, v. 63, p. 25-38.

Zhu, X., Samy, E., Russel, T., Altan, S., Hansen, L., and Yuan, J., 2001, Tomostatics applications for basalt-outcrop land and OBC multi-component surveys: Explor. Geophys., v. 32, p. 313-315.